

# Resonant Waveguide Grating Biosensors Based on Label-free Optical Principle

Igor Sallai<sup>1\*</sup>

<sup>1</sup> Nanobiosensorics Laboratory, Center of Energy Research, Eötvös Loránd Research Network, Konkoly-Thege Miklós út 29–33., H-1121 Budapest, Hungary

\* Corresponding author, e-mail: [sallai.igor@edu.bme.hu](mailto:sallai.igor@edu.bme.hu)

Received: 25 June 2023, Accepted: 18 July 2023, Published online: 22 September 2023

## Abstract

Label-free optical biosensors are powerful tools for the real-time monitoring of both molecular and cellular-scale interactions. Resonant waveguide grating biosensors are based on the detection of refractive index changes induced by molecular interactions and/or cell mass redistributions. The Epic BenchTop and Epic Cardio are two biosensors with high sensitivity and throughput that offer excellent potential for life science research. Both instruments are suitable for cell-based and biochemical assays. In this paper, I describe the principles of operation and performance of the Epic BenchTop and Epic Cardio label-free waveguide grating biosensors and discuss their applications in various research areas.

## Keywords

evanescent field, molecular interactions, waveguide grating

## 1 Introduction

With the growing need for rapid and accurate detection of materials, the development and design of high-sensitivity biosensors came to the foreground from the mid-20<sup>th</sup> century onwards. Biosensors are analytical tools that enable molecular interactions and cellular analysis at high resolution from small sample volumes. Optical biosensors include surface plasmon resonance sensors, light scattering optical sensors, fluorescence sensors, and optical waveguide sensors [1]. Optical biosensors, a popular class of biosensors, are gaining popularity because they allow measurements to be made without modification of biological samples [2]. Among their many advantages, perhaps the most important is their high sensitivity and speed of measurement. The technology enables the integration of passive and active components on the same substrate, providing miniaturization, robustness, reliability, mass production, low power consumption, and easy alignment of individual optical components [3].

## 2 Physical background of the sensing of resonant waveguide grating biosensors

The resonant waveguide grating biosensors are capable of guiding the wavelength component of illuminating light at resonant frequency in their thin, high refractive index

layers. As soon as the illuminating light hits the surface of the microtiter plate, a wavelength component with a resonant frequency (resonant wavelength) penetrates the thin waveguide layer. The resonance frequency wavelength component for the empty microtiter plate is 828.2 nm [4]. Within the waveguide layer, the incident light undergoes full reflection at the interfaces, but its phase is nevertheless shifted. Light beams coupled to the same grating interfere, but only positive interference causes waveguiding. This phenomenon is often called as constructive interference, which ensures that the incident wavelength component propagates for a short time in the waveguide layer (Fig. 1). The light reflected from the interface of the liquid containing the analyte and the waveguide layer forms an exponentially decreasing electromagnetic field, called the evanescent field [5, 6]. The evanescent field penetrates the 150–200 nm thick region of the suspension in contact with the surface. In practice, therefore, the local environment of the biosensor is called the evanescent field, which is formed in the 150–200 nm thickness of its surface. By increasing the angle of incidence of the illuminating light, the vertical extent of the evanescent field can be increased.

Detection of the wavelength component at the resonant frequency precipitated from the waveguide layer is

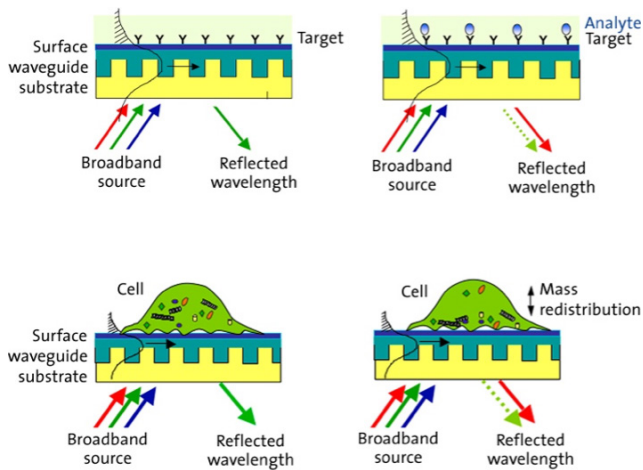


Fig. 1 Measurement scheme for label-free testing with resonant waveguide grating optical biosensors [6]

achieved using a complementary metal-oxide semiconductor (CMOS) camera (Figs. 2 and 3) [7–9].

### 3 Relationship between resonance peak and quality factor

The resonance peak defines how much light is reflected or transmitted by the biosensor at different wavelengths [10]. The full width at half maximum (FWHM) characterizes the resonance peak; it describes how sharp or narrow the resonance peak is [11]. A smaller FWHM means a sharper peak and higher sensitivity. For the characterization of resonant waveguide grating biosensors, a so-called quality factor can be introduced, which defines the ability of the biosensor to distinguish the smallest changes in the sample that cause a refractive index change. The quality factor can be calculated as the ratio of the resonant wavelength to the FWHM [12]. The quality factor can be improved by tuning the operating wavelength and the angle of incidence of the light source, among other things. This can change the coupling efficiency in the waveguide layer [13].

### 4 Grating designs, nanofabrication machining processes

Resonant waveguide grating (RWG) biosensors can have multiple grating geometries, the design of which requires the application of various nanofabrication machining techniques [14].

Holographic lithography is a technique that uses laser beams to create patterns on photosensitive materials [15]. Depending on the interference of the laser beams, the patterns can have different shapes and sizes.

Electron-beam lithography is another technique that uses electron beams to form patterns on machined surfaces. It is useful for creating non-periodic patterns that holographic lithography cannot. Electron beam

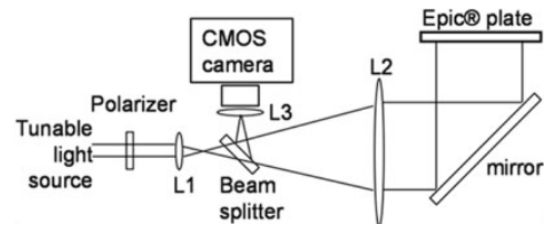


Fig. 2 Structural diagram of the Epic BT and Epic Cardio biosensors [8, 9]©

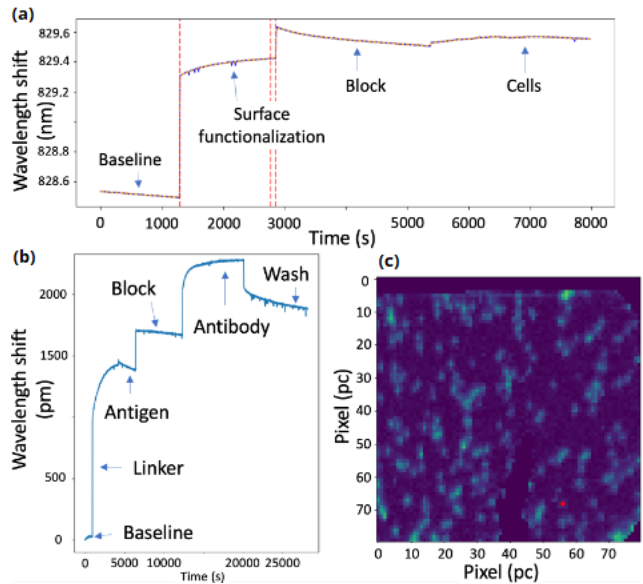


Fig. 3 Output data of the RWG biosensor; (a) shows an example of a set of wavelength shift events averaged over a single microtiter plate hole. The procedures and surface treatment/functionalization methods used at each stage are marked in the diagram; (b) shows a set of wavelength shift events occurring on a single sensor pixel; (c) shows a 25 μm resolution image taken with a CMOS camera, with the red marker indicating the cell just detected. The diagrams and CMOS recording in the figure present my own results

lithography can be used to create very fine lines. However, it can also cause errors when the aim is to join different parts of the pattern in large samples. However, some recent developments have improved the speed and quality of electron beam lithography [16].

In laser ablation, a laser can be used to create patterns on different materials. It allows patterns to be made directly on the surface without etching. Patterns can be made in parallel or sequentially. Laser ablation can also be used to create very small patterns of different depths. It can also leave debris particles around the pattern. The quality of laser ablation can be improved by using a special type of laser and a grating interferometer setup [17].

Deposition techniques are methods to create layers of material on a surface. These layers can affect the properties of the light passing through them. Different deposition techniques have different advantages and challenges.

Some techniques can create layers of different thicknesses or angles depending on the situation [18]. The deposition rate can vary depending on the experimental conditions.

Nanoimprint lithography (NIL) is a technique to copy nanostructures from a mould onto a surface [19]. This can be done in several ways, using heat, light, or soft materials. NIL can be used to create nanostructures quickly and cheaply. Some versions of NIL can change the size, shape or material of the nanostructures. Fig. 4 (b) shows an example of a  $\text{TiO}_2$  nanostructure fabricated by NIL machining [14].

### 5 The importance of RWG technology and refractive index monitoring

The label-free resonant waveguide grating (RWG) biosensors are designed to be optimized for high-resolution measurements of wavelength shift phenomena. The technology is based on the measurement of the change in refractive index, or local density, which is influenced by several biophysical parameters. The refractive index (RIU) is a non-dimensional quantity, which can be interpreted as the ratio of the speed of light measured in a vacuum to the speed of light measured in each medium [20].

A wide range of physical, chemical, and biological events can induce refractive index variations and hence induce the wavelength shift phenomena in RWG setups. In the following, I will highlight the most important of these phenomena. Chemical composition is a determining factor, for example, substances with a higher atomic or molecular density tend to have a higher refractive index. The refractive index of a material can vary with temperature [21]. Generally, a higher refractive index can be measured at lower temperatures, so proper incubation of the measuring equipment and the sample is essential. The wavelength of the illuminating light can also be influenced. This phenomenon is called dispersion. Dispersion is also responsible for the chromatic aberration in optical lenses [22]. The system pressure, or atmospheric pressure, is also a factor worth mentioning, as it can modify the refractive index value through the photoelastic

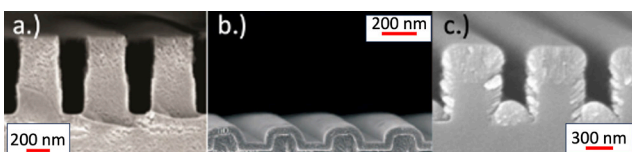


**Fig. 4** Scanning electron microscopic pictures of some commonly used gratings; (a) SiN grating; (b) replicated grating on  $\text{TiO}_2$ -coated polycarbonate; (c)  $\text{TiO}_2$  grating prepared by the NIL technique [14]©

phenomenon, which is often exploited in common pressure measurement devices [23, 24]. The electric and magnetic fields are also such factors, which can modify the local refractive index value through the electro-optical and magneto-optical effects [24].

### 6 Epic BenchTop and EPIC Cardio RWG biosensors

The technology, developed by Epic Corning Incorporated (Corning, NY, USA), consists of two main parts: the microtiter plates and an instrument containing the optical elements and the light source that provides the illumination.

The microtitre plate-based technology allows high-throughput experiments to be performed. The company sells 96, 384 and 1536-well plates (Society for Biomolecular Screening) (Fig. 5) [25].

Each well of the plates has a sensor area of  $2000 \mu\text{m} \times 2000 \mu\text{m}$ . As one moves from the sensor surface towards each layer, one encounters a highly refractive waveguide dielectric layer of niobium pentoxide ( $\text{Nb}_2\text{O}_5$ ), which, in addition to many advantageous optical properties, also imparts biocompatibility to the layer. The waveguide layer rests on a thicker substrate, which has a lower refractive index than the waveguide layer but a higher refractive index for proteins or other biological samples bound to the sensor surface [26]. Glass substrates are the most widely used. An integral part of the sensor is also the optical grating, which is embedded in the waveguide layer. The optical grating allows the illuminating light to penetrate the waveguide layer, nevertheless forming separate biosensors.

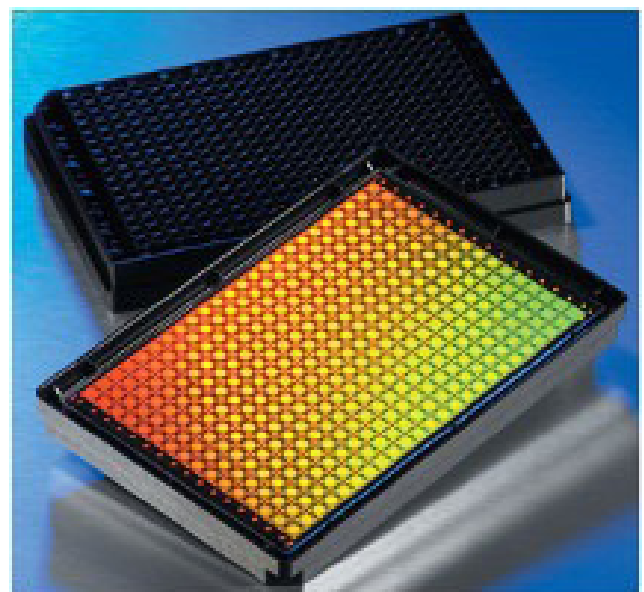


**Fig. 5** The 384-well Corning® Epic Biochemical Assay microtiter plate [25]

The technology uses a tuneable light source to simultaneously illuminate each sensor sheet of the plate. The light source emits light over a broad wavelength range, which is passed through a high-precision, narrow-pass optical filter that allows only the 823 to 838 nm wavelength range to be penetrated. The transmitted light can scan the microtiter plate every 20 ms and every 100  $\mu\text{m}$  [4, 7].

The EpicBT and Epic Cardio are easy-to-use, even portable, instruments with a compact design. Due to their simplified design, they contain a minimal number of moving parts and thus rarely require maintenance. Other advantages include a compact design that requires little space and can even be placed in an incubator. Both instruments can detect wavelength shift events in the 15000  $\text{pm}$  wavelength range with a resolution of 0.25  $\text{pm}$  [7, 27].

In the ELKH EK MFA Nanobiosensorics Research Group, led by Dr. Robert Horvath, experiments are also being carried out with label-free biosensors based on optical principles. The research group has a prototype instrument from Corning Inc. (USA), the Epic Cardio RWG biosensor, which is currently not yet commercially available. The name Cardio derives from the fact that it has also been used to study cardiotoxic compounds [28]. The instrument offers the possibility to study small molecule biochemistry, molecular and cellular biology phenomena due to its unique spatial and temporal resolution. It has a maximum spatial resolution of 25  $\mu\text{m}$  and a maximum temporal resolution of 3 s, while its resolution can be increased by manually positioning its internal optical elements, the lenses [5]. The team has developed a microtiter plate positioning conditioner (Fig. 6) and an IT platform for the interpretation and interpretation of wavelength shift signals and dynamic mass redistribution phenomena. Other developments of the research group include various fluid handling techniques that can be fitted to sensors, as well as flow cuvettes and rotating flow field arrays [5, 29].

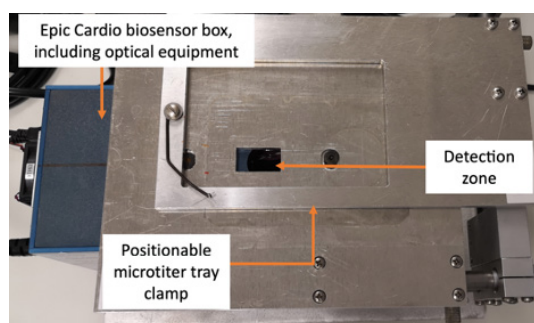


**Fig. 6** The Epic Cardio RWG biosensor and the positional microtiter plate holder developed by the Nanobiosensorics Research Group

One of the advantages of EpicBT is that it can analyze every single well of a plate at the same time, whereas with Epic Cardio only 12 wells can be analyzed at a time in a  $3 \times 4$  arrangement (Fig. 7). For Epic BT, a maximum temporal resolution of 3 s and a spatial resolution of 83  $\mu\text{m}$  can be achieved [4] (Fig. 7). Individual components appearing on the sensor surface can be detected from the analyte with a minimum surface density of up to 0.078  $\text{ng}/\text{cm}^2$  [4, 30]. The Aligner software allows the averaged wavelength shift in each well to be monitored in real time during the measurement (Fig. 3).

### 7 The Corning Epic System

The Epic Cardio and BT is an improved, incubate, simultaneous, multi-plate inspection system for the Corning Epic System [31, 32]. It is a unique, semi-automated system consisting of a temperature control unit, an optical apparatus, and a robotic fluid handling unit. By incorporating a temperature control unit, it is possible to eliminate baseline fluctuations due to temperature fluctuations. The system can be divided into two units: the biosensor microtiter plates and the system of microtiter plates for storing the components added during the experiment: cell suspension, protein solution and washing liquid. During the measurement with the system, after temperature stabilization, the sensing plate is transferred by a robotic arm to the plate storage unit located above the detection apparatus, and then the components required for the measurement are dispensed from the corresponding well of the analyte-containing plate into each well of the biosensor plate by a liquid handling unit [31]. The automated dispensing of each

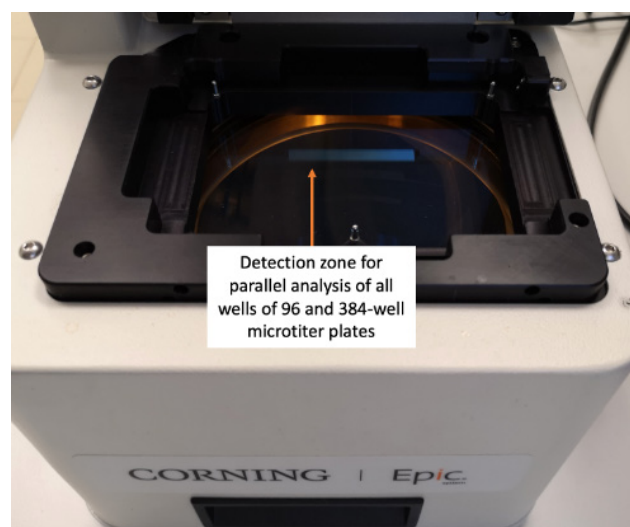


**Fig. 7** Epic BT RWG biosensor used by the Nanobiosensorics Lendület Research Group

analyte can be programmed, and the measurement can be monitored in real-time. The dosing of the cell suspension must always be performed manually.

### 8 The RWG technology potential in cellular science

The previously mentioned wavelength shifts are basically generated by dynamic mass redistribution (DMR) events at the sensor surface. Redistribution is the result of translocations at the sensor surface, which can result from molecular interactions at a given point on the sensor surface, new bond formation, bond breaking, and washing off certain components [33]. The interaction of cells immobilized on the sensor surface with drug molecules and endotoxins can be investigated [34]. Interaction-induced cytoplasmic rearrangements modify the local refractive index of the sensor. G protein-coupled receptor responses induced by some agonist and antagonist drug substances have been shown to be measurable by cell surface mass transfer [31]. By monitoring dynamic redistribution, even motor protein (e.g., actin, tubulin) rearrangements induced by drug substances or surface attachment of peptides of a few amino acids in length can be measured [33]. These phenomena may include the most feasible physisorption. Simple physisorption occurs, for example, during the surface attachment of antibodies. The surface of the biosensor can be functionalized with different ligands, polymers, antibodies, or antigens to exploit the potential of physisorption. The functionalization of the surface depends of course on the experiment: in many cases, the aim is to efficiently dock cells to study the effect of a drug substance on as many cells as possible. For example, PLL-g-PEG (a copolymer of poly-L-lysine and polyethylene glycol graft), which can be functionalized to ensure a thorough attachment of living cells to the surface [7], can be used. However, if the aim is to study cell activation, antigens, antibodies, receptor-binding ligands, and other molecules specific to different signaling pathways are attached to the surface. Either spreading during surface adhesion of a single cell or the release of vesicles, exocytotic granules can be studied.

In a prominent study by the Nanobiosensorics Research Group, Epic Cardio and Epic BT biosensors were used to measure the adhesion properties of cancer cells [35, 36]. Using HeLa cells as model organisms, they demonstrated that the glycocalyx structure of the cells significantly influences the strength of cell adhesion to RGD (arginine-glycine-aspartic acid) peptide-coated surfaces and the kinetics of cell outgrowth [35]. The glycocalyx structure of the cells was hydrolyzed and the adhesion kinetics of intact

cells and hydrolyzed cells were compared [35]. Chondroitin sulfate, an important component of the glycocalyx layer, was digested by chondroitinase ABC enzyme. Lognormal curves could be fitted to the maximum wavelength shift values measured during adhesion of individual cells [36]. These studies confirmed that the presence or absence of the glycocalyx structure can have far-reaching consequences on the adhesion properties of cancer cells. The studies confirm that further research is needed to develop more reliable and effective cancer drugs that affect adhesion.

### 9 Comparison of RWG biosensors with other biosensors

Optical biosensors enable single-cell studies. Each biosensor can be compared in terms of invasiveness, permeability, the origin of the biosensor output signals and the principle of operation [34].

Both Surface Plasmon Resonance (SPR) and RWG with or without microfluidics are considered non-invasive and measure the change in local refractive index. Electrical biosensors, Surface Acoustic Wave (SAW) biosensors and Quartz Crystal Microbalance with Dissipation (QCM-D) biosensors all use electrical input signals and are thus minimally invasive [34, 37, 38]. SAW technology allows the measurement of acoustic wave propagation along the surface of the applied piezoelectric crystal [39]. QCM-D technology allows the measurement of the strength of interactions between the functionalized sensor surface and individual nanoparticles through the measurement of dissipation and frequency [40]. The QCM-D and SAW are all low throughput biosensors, while the RWG biosensors allow the analysis of microplates with up to 1536 wells [41–43]. In general, all biosensors are mostly sensitive to cell-analyte interactions. SPR, RWG, SAW and QCM-D generally have a sensing depth of 100–200 nm, while infrared SPR and electrical biosensors have a sensing depth greater than this [34, 38, 44]. The sensitivity of the sensors can also be used to compare the technologies in use. With RWG technology, a detection limit of ng/mL can be achieved, as reported by Paulsen et al. in their paper, where they successfully detected CD40 ligand antibody at concentrations as low as 24 ng/mL [45]. Measurements of mass per unit area can be in the ng/cm<sup>2</sup> range for RWG sensors, which can approximate QCM and SAW sensors to a similar order of magnitude. The RWG and SAW technology allows the detection of antigen-antibody interactions at a surface mass density of 0.1–10 ng/cm<sup>2</sup> while this value is around 0.01–100 ng/cm<sup>2</sup> for QCM [46, 47]. The output

signal is sensor-dependent, both RWG and SPR measure DMR resulting from interactions at the sensor surface, which may originate from adhesion interactions or from changes in cytoskeletal structure and cell morphology.

### 10 The future of Epic Cardio and EpicBT

Increasing the spatial resolution of biosensors could be the future direction of development. One possible solution to increase the spatial resolution of RWG biosensors is to incorporate smaller electrodes or more electrodes per well of a microtiter plate. However, this requires modification of the biosensor system hardware and software, which is not always a cost-effective solution. Munteanu et al. describe a method to increase the spatial resolution of an electrochemical sensor in combination with optical microscopy [48]. The authors developed electrochemical biosensors for the detection of hydrogen peroxide and glucose by drop-casting enzyme and redox polymer mixtures onto planar, optically transparent electrodes. These biosensors generate current signals proportional to the concentration of the analyte through a series of reactions that ultimately change the oxidation state of the redox polymer. Images of the interfaces of these biosensors were obtained by Bright Field Reflection Light Microscopy (BFRLM). The study showed that the intensity of the images is higher when the redox polymer is in the oxidized state than when it is in the reduced state. It was also found that the time required for the redox polymer to change its oxidation state can be determined optically and depends on the concentration of the analyte.

### References

- [1] Damborský, P., Švitel, J., Katrlík, J. "Optical biosensors", *Essays in Biochemistry*, 60(1), pp. 91–100, 2016.  
<https://doi.org/10.1042/EBC20150010>
- [2] Zourob, M., Lakhtakia, A. (eds.) "Optical Guided-wave Chemical and Biosensors I", Springer, 2009. ISBN 978-3-540-88241-1  
<https://doi.org/10.1007/978-3-540-88242-8>
- [3] Zinoviev, K., Carrascosa, L. G., del Río, J. S., Sepúlveda, B., Domínguez, C., Lechuga, L. M. "Silicon photonic biosensors for lab-on-a-chip applications", *Advances in Optical Technologies*, 2008, 383927, 2008.  
<https://doi.org/10.1155/2008/383927>
- [4] Orgovan, N., Kovacs, B., Farkas, E., Szabó, B., Zaytseva, N., Fang, Y., Horvath, R. "Bulk and surface sensitivity of a resonant waveguide grating imager", *Applied Physics Letters*, 104(8), 083506, 2014.  
<https://doi.org/10.1063/1.4866460>
- [5] Sztilkovics, M., Gerecsei, T., Peter, B., Saftics, A., Kurunzi, S., Szekacs, I., Szabo, B., Horvath, R. "Single-cell adhesion force kinetics of cell populations from combined label-free optical biosensor and robotic fluidic force microscopy", *Scientific Reports*, 10(1), 61, 2020.  
<https://doi.org/10.1038/s41598-019-56898-7>
- [6] Biocompare "Innovations in Label-Free Detection", *Biocompare*, Nov. 13., 2018. [online] Available at: <https://www.biocompare.com/Editorial-Articles/354149-Innovations-in-Label-Free-Detection/> [Accessed: 23 October 2022]
- [7] Orgovan, N., Peter, B., Bösze, S., Ramsden, J. J., Szabó, B., Horvath, R. "Dependence of cancer cell adhesion kinetics on integrin ligand surface density measured by a high-throughput label-free resonant waveguide grating biosensor", *Scientific Reports*, 4(1), 4034, 2014.  
<https://doi.org/10.1038/srep04034>

- [8] Fang, Y. "Resonant waveguide grating imagers for single cell analysis and high throughput screening", In: *Biosensing and Nanomedicine VIII*, San Diego, CA, USA, 2015, 95500P. ISBN 9781628417166  
<https://doi.org/10.1117/12.2190287>
- [9] Febles, N. K., Chandrasekaran, S., Fang, Y. "Resonant waveguide grating imager for single cell monitoring of the invasion of 3D Spheroid cancer cells through Matrigel", In: Rasooly, A., Prickril, B. (eds.) *Biosensors and Biodetection: Methods and Protocols Volume 1: Optical-Based Detectors*, Humana Press, 2017, pp. 143–160. ISBN 978-1-4939-6846-6  
[https://doi.org/10.1007/978-1-4939-6848-0\\_10](https://doi.org/10.1007/978-1-4939-6848-0_10)
- [10] Kovacs, B., Kraft, F. A., Szabo, Z., Nazirzadeh, Y., Gerken, M., Horvath, R. "Near cut-off wavelength operation of resonant waveguide grating biosensors", *Scientific Reports*, 11(1), 13091, 2021.  
<https://doi.org/10.1038/s41598-021-92327-4>
- [11] Hiremath, K. R. "Coupled mode theory based modeling and analysis of circular optical microresonators", PhD Thesis, University of Twente, 2005. [online] Available at: <https://research.utwente.nl/en/publications/coupled-mode-theory-based-modeling-and-analysis-of-circular-optic> [Accessed: 24 June 2023]
- [12] Fang, Y., Ferrie, A. M., Fontaine, N. H., Mauro, J., Balakrishnan, J. "Resonant waveguide grating biosensor for living cell sensing", *Biophysical Journal*, 91(5), pp. 1925–1940, 2006.  
<https://doi.org/10.1529/biophysj.105.077818>
- [13] Shi, Q., Liang, L., Zhao, J. "Joint optimization of quality factor and sensitivity: Research on the performance quantification of two dimensional photonic crystal biosensor", *Optik*, 245, 167657, 2021.  
<https://doi.org/10.1016/j.ijleo.2021.167657>
- [14] Quaranta, G., Basset, G., Martin, O. J. F., Gallinet, B. "Recent Advances in Resonant Waveguide Gratings", *Laser & Photonics Reviews*, 12(9), 1800017, 2018.  
<https://doi.org/10.1002/lpor.201800017>
- [15] Lu, C., Lipson, R. H. "Interference lithography: A powerful tool for fabricating periodic structures", *Laser & Photonics Reviews*, 4(4), pp. 568–580, 2010.  
<https://doi.org/10.1002/lpor.200810061>
- [16] Finot, E., Bourillot, E., Meunier-Prest, R., Lacroute, Y., Legay, G., Cherkaoui-Malki, M., Latruffe, N., Siri, O., Braunstein, P., Dereux, A. "Performance of interdigitated nanoelectrodes for electrochemical DNA biosensor", *Ultramicroscopy*, 97(1–4), pp. 441–449, 2003.  
[https://doi.org/10.1016/S0304-3991\(03\)00072-X](https://doi.org/10.1016/S0304-3991(03)00072-X)
- [17] Singh, S., Argument, M., Tsui, Y. Y., Fedosejevs, R. "Effect of ambient air pressure on debris redeposition during laser ablation of glass", *Journal of Applied Physics*, 98(11), 113520, 2005.  
<https://doi.org/10.1063/1.2138800>
- [18] Saleem, M. R., Ali, R., Bilal Khan, M., Honkanen, S., Turunen, J. "Impact of atomic layer deposition to nanophotonic structures and devices", *Frontiers in Materials*, 1, 18, 2014.  
<https://doi.org/10.3389/fmats.2014.00018>
- [19] Muehlberger, M. "Nanoimprinting of Biomimetic Nanostructures", *Nanomanufacturing*, 2(1), pp. 17–40, 2022.  
<https://doi.org/10.3390/nanomanufacturing2010002>
- [20] Gómez-Castaño, M., Garcia-Pomar, J. L., Pérez, L. A., Shanmugathan, S., Ravaine, S., Mihi, A. "Electrodeposited Negative Index Metamaterials with Visible and Near Infrared Response", *Advanced Optical Materials*, 8(19), 2000865, 2020.  
<https://doi.org/10.1002/adom.202000865>
- [21] Abbate, G., Bernini, U., Ragozzino, E., Somma, F. "The temperature dependence of the refractive index of water", *Journal of Physics D: Applied Physics*, 8(11), 1167, 1978.  
<https://doi.org/10.1088/0022-3727/11/8/007>
- [22] Benedi-Garcia, C., Vinas, M., Dorronsoro, C., Burns, S. A., Peli, E., Marcos, S. "Vision is protected against blue defocus", *Scientific Reports*, 11(1), 352, 2021.  
<https://doi.org/10.1038/s41598-020-79911-w>
- [23] Morizet, J., Olivier, N., Mahou, P., Boutillon, A., Stringari, C., Beaupaire, E. "Third harmonic imaging contrast from tubular structures in the presence of index discontinuity", *Scientific Reports*, 13(1), 7850, 2023.  
<https://doi.org/10.1038/s41598-023-34528-7>
- [24] Singh, A. K., Mittal, S., Das, M., Saharia, A., Tiwari, M. "Optical biosensors: a decade in review", *Alexandria Engineering Journal*, 67, pp. 673–691, 2023.  
<https://doi.org/10.1016/j.aej.2022.12.040>
- [25] SelectScience "Corning® Epic® 384-well Biochemical Assay Microplate by Corning Life Sciences", [online] Available at: <https://www.selectscience.net/products/corning-epic-384-well-biochemical-assay-microplate/?prodID=198255> [Accessed: 23 October 2022]
- [26] Horváth, R., Lindvold, L. R., Larsen, N. B. "Reverse-symmetry waveguides: Theory and fabrication", *Applied Physics B*, 74(4), pp. 383–393, 2002.  
<https://doi.org/10.1007/s003400200823>
- [27] Shamah, S. M., Cunningham, B. T. "Label-free cell-based assays using photonic crystal optical biosensors", *Analyst*, 136(6), pp. 1090–1102, 2011.  
<https://doi.org/10.1039/c0an00899k>
- [28] Ferrie, A. M., Wu, Q., Deichmann, O. D., Fang, Y. "High frequency resonant waveguide grating imager for assessing drug-induced cardiotoxicity", *Applied Physics Letters*, 104(18), 183702, 2014.  
<https://doi.org/10.1063/1.4876095>
- [29] Kovács, K. D., Novák, M., Hajnal, Z., Hős, C., Szabó, B., Székács, I., Fang, Y., Bonyár, A., Horvath, R. "Label-free tracking of whole-cell response on RGD functionalized surfaces to varied flow velocities generated by fluidic rotation", *Journal of Colloid and Interface Science*, 599, pp. 620–630, 2021.  
<https://doi.org/10.1016/j.jcis.2021.04.091>
- [30] Peter, B., Farkas, E., Forgacs, E., Saftics, A., Kovacs, B., Kurunczi, S., Szekacs, I., Csampai, A., Bosze, S., Horvath, R. "Green tea polyphenol tailors cell adhesivity of RGD displaying surfaces: Multicomponent models monitored optically", *Scientific Reports*, 7(1), 42220, 2017.  
<https://doi.org/10.1038/srep42220>
- [31] Li, G., Ferrie, A. M., Fang, Y. "Label-Free Profiling of Ligands for Endogenous GPCRs Using a Cell-Based High-Throughput Screening Technology", *JALA: Journal of the Association for Laboratory Automation*, 11(4), pp. 181–187, 2006.  
<https://doi.org/10.1016/j.jala.2006.06.001>
- [32] Schröder, R., Schmidt, J., Blättermann, S., Peters, L., Janssen, N., Grundmann, M., Seemann, W., Kaufel, D., Merten, N., Drewke, C., Gomeza, J., Milligan, G., Mohr, K., Kostenis, E. "Applying label-free dynamic mass redistribution technology to frame signaling of G protein-coupled receptors noninvasively in living cells", *Nature Protocols*, 6(11), pp. 1748–1760, 2011.  
<https://doi.org/10.1038/nprot.2011.386>

- [33] Dagestani, H. N., Day, B. W. "Theory and Applications of Surface Plasmon Resonance, Resonant Mirror, Resonant Waveguide Grating, and Dual Polarization Interferometry Biosensors", *Sensors*, 10(11), pp. 9630–9646, 2010.  
<https://doi.org/10.3390/s101109630>
- [34] Fang, Y. "Label-Free Biosensor Methods in Drug Discovery", Humana Press, 2015. ISBN 978-1-4939-2616-9  
<https://doi.org/10.1007/978-1-4939-2617-6>
- [35] Kanyo, N., Kovacs, K. D., Saftics, A., Szekacs, I., Peter, B., Santa-Maria, A. R., Walter, F. R., Dér, A., Deli, M. A., Horvath, R. "Glycocalyx regulates the strength and kinetics of cancer cell adhesion revealed by biophysical models based on high resolution label-free optical data", *Scientific Reports*, 10(1), 22422, 2020.  
<https://doi.org/10.1038/s41598-020-80033-6>
- [36] Kanyo, N., Kovacs, K. D., Kovacs, S. V., Béres, B., Peter, B., Székács, I., Horvath, R. "Single-cell adhesivity distribution of glyco-calyx digested cancer cells from high spatial resolution label-free biosensor measurements", *Matrix Biology Plus*, 14, 100103, 2022.  
<https://doi.org/10.1016/j.mbplus.2022.100103>
- [37] Sun, H., Wei, Y., Deng, H., Xiong, Q., Li, M., Lahiri, J., Fang, Y. "Label-free cell phenotypic profiling decodes the composition and signaling of an endogenous ATP-sensitive potassium channel", *Scientific Reports*, 4(1), 4934, 2014.  
<https://doi.org/10.1038/srep04934>
- [38] Wong, S.-H., Gao, A., Ward, S., Henley, C., Lee, P. H. "Development of a label-free assay for sodium-dependent phosphate transporter NaPi-IIb", *SLAS Discovery*, 17(6), pp. 829–834, 2012.  
<https://doi.org/10.1177/1087057112442961>
- [39] Mandal, D., Banerjee, S. "Surface Acoustic Wave (SAW) Sensors: Physics, Materials, and Applications", *Sensors*, 22(3), 820, 2022.  
<https://doi.org/10.3390/s22030820>
- [40] Chen, Q., Xu, S., Liu, Q., Masliyah, J., Xu, Z. "QCM-D study of nanoparticle interactions", *Advances in Colloid and Interface Science*, 233, pp. 94–114, 2016.  
<https://doi.org/10.1016/j.cis.2015.10.004>
- [41] Yashunsky, V., Lirtsman, V., Golosovsky, M., Davidov, D., Aroeti, B. "Real-time monitoring of epithelial cell-cell and cell-substrate interactions by infrared surface plasmon spectroscopy", *Biophysical Journal*, 99(12), pp. 4028–4036, 2010.  
<https://doi.org/10.1016/j.bpj.2010.10.017>
- [42] Chen, J. Y., Shahid, A., Garcia, M. P., Penn, L. S., Xi, J. "Dissipation monitoring for assessing EGF-induced changes of cell adhesion", *Biosensors and Bioelectronics*, 38(1), pp. 375–381, 2012.  
<https://doi.org/10.1016/j.bios.2012.06.018>
- [43] Saitakis, M., Gizeli, E. "Acoustic sensors as a biophysical tool for probing cell attachment and cell/surface interactions", *Cellular and Molecular Life Sciences*, 69(3), pp. 357–371, 2012.  
<https://doi.org/10.1007/s00018-011-0854-8>
- [44] Fang, Y. "Label-Free Biosensors for Cell Biology", *International Journal of Electrochemistry*, 2011, 460850, 2011.  
<https://doi.org/10.4061/2011/460850>
- [45] Paulsen, M., Jahns, S., Gerken, M. "Intensity-based readout of resonant-waveguide grating biosensors: Systems and nanostructures", *Photonics Nanostructures - Fundamentals and Applications*, 26, pp. 69–79, 2017.  
<https://doi.org/10.1016/j.photonics.2017.07.003>
- [46] Ba Hashwan, S. S., Khir, M. H. M., Nawi, I. M., Ahmad, M. R., Hanif, M., Zahoor, F., Al-Douri, Y., Algamili, A. S., Bature, U. I., Alabsi, S. S., Sabbea, M. O. B., Junaid, M. "A review of piezoelectric MEMS sensors and actuators for gas detection application", *Discover Nano*, 18(1), 25, 2023.  
<https://doi.org/10.1186/s11671-023-03779-8>
- [47] Glassford, A. P. M., Garrett, J. W., Bowers, W. D. "Mass sensitivity calibration of the surface acoustic wave quartz crystal microbalance (SAW QCM) at ambient temperature", *Proceedings of SPIE: Optical System Contamination: Effects, Measurements, and Control IV*, 2261, pp. 284–299, 1994.  
<https://doi.org/10.1117/12.190149>
- [48] Munteanu, R.-E., Ye, R., Polonschii, C., Ruff, A., Gheorghiu, M., Gheorghiu, E., Boukherroub, R., Schuhmann, W., Melinte, S., Gáspár, S. "High spatial resolution electrochemical biosensing using reflected light microscopy", *Scientific Reports*, 9(1), 15196, 2019.  
<https://doi.org/10.1038/s41598-019-50949-9>